Supramolecular Structures of Zinc (II) (8-Quinolinolato) Chelates†

Linda S. Sapochak,*,‡ Anna Falkowitz,§ Kim F. Ferris,‡ Spencer Steinberg,§ and Paul E. Burrows‡

Division of Materials Science, Pacific Northwest National Laboratory, Richland, Washington 99352, Department of Chemistry, University of Nevada, Las Vegas, Nevada 89154-4003

Received: October 10, 2003; In Final Form: February 5, 2004

We investigate the oligomeric purity and stability of zinc (8-quinolinolato) (Znq_2) and its methylated derivatives (nMeq$_2$Zn, $n = 2, 4, 5$) through a combination of theoretical modeling of oligomerization energetics leading to supramolecular structures and experimental size-exclusion chromatography studies. Gas- and solution-phase ($CHCl_3$) formation energies for dimeric, trimeric, and tetrameric species are reported. Favorable gas-phase thermodynamics were calculated and found to favor tetrameric structures for all Znq_2 chelates (~ -50 kcal/mol for monomer dimerization to ~ -35 kcal/mol for dimer dimerization), with the exception of 2Meq$_2$Zn, which gave lower formation energies by 30−45% due to steric hindrance. Solvation model computations indicate that these energies are reduced by ~10−25% with the introduction of a dielectric medium. Computed structural parameters for the basic Zn−O core structure formed via bridging of phenolato oxygens do not change significantly as oligomer growth progresses. Size-exclusion chromatography experiments of crystalline and amorphous films (vapor deposited) dissolved in $CHCl_3$ or $CHCl_3$/DMSO mixtures showed that the dominant species for Znq_2, 4Meq$_2$Zn, and 5Meq$_2$Zn is tetrameric, but partial disassociation to monomers can occur in the presence of nucleophilic solvent. The sterically hindered 2Meq$_2$Zn was monomeric in all solvent systems. Implications for organic light-emitting devices using these materials are discussed.

1. Introduction

Metal chelates of 8-quinolinol have been the subject of renewed interest since the demonstration of their use in low-voltage organic light-emitting devices (OLEDs).[1] Many detailed studies of the molecular and electronic structure of aluminum tris(8-quinolinolato) (Alq_3)[2−6] and its substituted derivatives[7,8] have been reported. Although Alq_3 is often referred to as the "archetypal" electroluminescent material, its structural diversity limits our ability to relate molecular structure to charge injection and mobility, a problem common to the metal trisquinolates. Geometric isomerization between meridianal (mer) and facial (fac) isomers of Alq_3 has been proposed[9,10] and several polymorphic phases identified,[2,11] suggesting that thin films deposited under different conditions may have structural variations that contribute to device property variations. To understand the basic physics of device operation and to develop structure−property relationships that will lead to design rules for improved molecules, materials with well-defined and controllable molecular structures in the solid state are necessary.

Recently, X-ray diffraction studies of zinc bis(8-quinolinolato) (Znq_2) have shown that the metal chelate forms a supramolecular tetrameric structure composed of a Zn_4O_8 core via oxo-bridging of the 8-quinolinolato ligands.[12,13] Unlike the metal trisquinolates, the Znq_2 tetramer exhibits no geometric isomerization and thermal analysis by differential scanning calorimetry (DSC) demonstrated a sole oligomeric species and no polymorphism.[13] The high symmetry of the supramolecular tetramer results in a near-zero molecular dipole moment, which may be an important factor in reducing dipolar disorder and charge trapping in solid-state films.[14] For example, comparison of identical, undoped devices grown using Alq_3 and $(Znq_2)_4$ as the emissive and electron-transport layer showed that the latter devices exhibited lower operating voltage; however, those results do not distinguish between injection-limited and bulk-limited conduction.[13] Study of the methylated derivatives is particularly interesting because the C4-methylated derivative of Alq_3, 4Meq$_3$Al, shows increased electroluminescence quantum efficiency,[7] and similar effects might be expected for the methylated Znq_2 derivative. However, solution photophysical studies suggest that methylated derivatives of Znq_2 may exist in different oligomeric forms.[15,16]

While there is clear evidence for the stability of the Znq_2 tetramer in the solid phase,[12,13] the detailed structure of the methylated derivatives is unknown. The formation of $(Znq_2)_4$ can be viewed as a sequence of oligomerization steps, each with individual reaction energetics. The manipulation and control of the relative energetics of each step affects the size and three-dimensional structure of the Zn−O core structure. It is also clear that solvation effects play an important role in the assembly of this supramolecular structure. For example, previous work by Hopkins et al., using solution ^{1}H NMR spectroscopy has indicated that the tetramer is the more probable form of Znq_2 in chloroform but partially dissociates to monomers in nucleophilic solvents such as DMSO.[8] There are other reports of zinc chelates that form larger structures via bridging oxygen atoms, which are affected by the experimental conditions, whether in solution or solid state. Van der Schaaf et al. has earlier reported synthesis of organo zinc complexes with 2-pyridylmethanolate ligands.[17] These compounds were the basic part of an oligomeric series which formed dimers to give a Zn_2O_2 four-membered-ring structure and trimers to give a Zn_3O_3 six-membered-ring structure, both with distorted tetrahedral geometries about the

† Part of the special issue "Alvin L. Kwiram Festschrift".

* Author to whom correspondence may be addressed. Fax: (509) 375-2186. E-mail: linda.sapochak@pnl.gov.

‡ Pacific Northwest National Laboratory.

§ University of Nevada.

10.1021/jp037074s CCC: $27.50
Published on Web 03/18/2004

zinc ions. In the latter case, the trimer species was identified in solution by NMR, but upon crystallization, X-ray diffraction showed the material to be "tetrameric", forming an eight-membered Zn_4O_4 ring structure. More recently, Yu et al. revealed the structure of the white-emitting electroluminescent material, zinc 2-(2-hydroxyphenyl)benzothiazolate (Zn_2BZT_4) to be dimeric,[18] and Kim et al. showed that zinc 2-(2-hydroxyphenyl)-5-phenyl-1,3-oxazolate formed both monomeric ($Znppo_2$) and trimeric [$(Znppo_2)_3$] structures.[19] In both cases, the oligomers were formed via bridging phenolato oxygens resulting in a Zn_2O_2 core structure similar to tetrameric Znq_2. Thus, while experimental evidence to date would indicate that Zn (8-quinolinolato) chelates should be tetrameric in the solid state, this extension may not be applicable to the solution phase, nor to the methylated derivatives. Clarification of these structures is essential in order to understand structure−property relationships in OLEDs made using these materials.

In this paper, we use a combination of electronic-structure calculations and experimental size characterization to examine the oligomeric purity of Znq_2 and its methylated derivatives nMeq$_2$Zn ($n = 2, 4, 5$), where the monomer form is used as the basic building block for developing $(n\text{Meq}_2\text{Zn})_x$ ($x = 1, 2, 3, 4$) supramolecular structures. Experimentally, the materials were examined using size-exclusion chromatography (SEC) of crystalline and vapor-deposited film samples dissolved in different solvents. We show that the tendency to form a tetrameric structure is thermodynamically favorable for all methylated derivatives.

2. Experimental Section

2.1. Computational Methods. Ab initio Hartree−Fock electronic-structure computations were performed for the $(Znq_2)_x$ and $(n\text{Meq}_2\text{Zn})_x$ series where x denotes the level of oligomerization ($x = 1, 2, 3, 4$) and n the derivatization site ($n = 2, 4, 5$) on the 8-quinolinol ligands using the GAMESS electronic-structure program.[20] Molecular geometries were force optimized at the SCF level using the 3-21G* basis set with C_1 symmetry.[21,22] Starting geometries for these optimizations were derived from the X-ray crystal structure of the unsubstituted parent compound $(Znq_2)_4$.[12] Estimated formation energies were defined as the difference between the total energies of the larger oligomer and the sum of the constituent Znq_2-based components. Gibbs free energies were estimated for the molecules in chloroform solvent using the integral equation formalism for the polarized continuum model (PCM) of Tomasi and coworkers.[23−26] Molecular geometries for PCM calculations were the gas-phase-optimized structures. A solvent-probe radius of 1.4 Å was used for the determination of the accessible surface area. Full coordinates of the computed compounds are given in the supplementary information.

2.2. Materials. The metal chelates Alq_3 and Znq_2 were obtained from Aldrich Chemical Co. Synthesis of nMeq$_2$Zn chelates ($n = 2, 4, 5$) has been reported elsewhere.[15,16] All metal chelate samples were purified by high vacuum gradient temperature sublimation as described previously.[16] Polystyrene molecular weight (MW) standards (760 and 2330 amu), 8-quinolinol (recrystallized from 95% ethanol), and 2,9-dimethyl-4,7−1,10 -phenanthroline (DDP) were obtained from Aldrich Chemical, Co.

2.3. SEC. Size-exclusion chromatography was performed using high-performance liquid chromatography (HPLC) equipment consisting of a B-100-S pump (Eldex Laboratories, Inc.), Rheodyne model 7725 injector with a 50-μL injector loop, an SSI model LP-21 pulse dampener, and a Shodex (RI-71) refractive index detector. All HPLC separations were performed on two 300 mm × 7.8 mm Jordi Gel polystyrene 100-Å size-exclusion columns placed in series (Alltech Associates, Inc.). The analytical columns were protected from contamination with a 50 mm × 10 mm guard column of the same material. Eluting compounds were detected and evaluated with an analogue to digital converter running "Simple Peak" software (SRI). Chloroform was used as the mobile phase (HPLC-grade chloroform, Aldrich). A small amount of DMSO (Burdick & Jackson) was added as a cosolvent for some of the analysis to measure the stability of metal chelates to nucleophilic solvents.

Samples (5 mg) of the crystalline material were dissolved in chloroform and diluted to 5.00 mL in a volumetric flask. The ligand, 8-hydroxyquinoline, Alq_3, and the polystyrene standards dissolved completely in chloroform, giving known concentrations of 1 mg/ml. However, standards of the nMeq$_2$Zn chelates were not prepared quantitatively because of limited solubility. Solutions of nMeq$_2$Zn, which failed to completely dissolve required filtration through a 0.2-μm filter before HPLC analysis. Thin films grown on quartz slides were obtained by thermal sublimation at a base pressure of $\sim 10^{-6}$ Torr and deposition rate of 1−2 Å/s. The thin film was subsequently dissolved off the slide with chloroform. For consistency, all samples were filtered in the same manner before injection on the column and run in duplicate. Samples prepared in chloroform/DMSO mixtures were prepared identically as described above, except 10 μL of DMSO was added as cosolvent after filtration in $CHCl_3$. HPLC analysis of the samples was conducted by injecting 25 μL at a flow rate of 0.80 mL/min. Nominal column back pressure during SEC analysis was 850−900 psi.

TABLE 1: Gas- and Solution-Phase Oligomerization Energies (kcal/mol) for $(n\text{Meq}_2\text{Zn})_x$ Chelates

oligomerization reaction	$(Znq_2)_x$	$(2\text{Meq}_2\text{Zn})_x$	$(4\text{Meq}_2\text{Zn})_x$	$(5\text{Meq}_2\text{Zn})_x$
$n\text{Meq}_2\text{Zn} + n\text{Meq}_2\text{Zn} \rightarrow (n\text{Meq}_2\text{Zn})_2$				
gas phase	−53.2	−36.1	−52.2	−53.7
solution ($CHCl_3$)	−43.9	−27.5	−46.6	−44.1
$n\text{Meq}_2\text{Zn} + (n\text{Meq}_2\text{Zn})_2 \rightarrow (n\text{Meq}_2\text{Zn})_3$				
gas phase	−47.4	−35.0	−46.4	−47.7
solution ($CHCl_3$)	−38.7	−27.5	−39.1	−38.6
$n\text{Meq}_2\text{Zn} + (n\text{Meq}_2\text{Zn})_3 \rightarrow (n\text{Meq}_2\text{Zn})_4$				
gas phase	−40.5	−22.8	−38.9	−40.4
solution ($CHCl_3$)	−32.4	−18.6	−33.8	−32.9
$(n\text{Meq}_2\text{Zn})_2 + (n\text{Meq}_2\text{Zn})_2 \rightarrow (n\text{Meq}_2\text{Zn})_4$				
gas phase	−34.8	−21.7	−33.1	−34.4
solution ($CHCl_3$)	−27.2	−18.5	−26.2	−27.4

3. Results

3.1. Calculated Structures and Energetics of the $(n\text{Meq}_2\text{Zn})_x$ Oligomerization Process. In this section, we report the oligomerization reaction energetics and electronic-structure calculations for $(Znq_2)_x$ and the $(n\text{Meq}_2\text{Zn})_x$ series and discuss in detail how the effects of ligand methylation influence the Zn−O core structure and corresponding reaction energetics for building supramolecular structures. Energetic values relating to the oligomerization process, as shown in Figure 1 are given in Table 1. While the computed energetics provide a general assessment of the overall reaction likelihood, individual steps of the reaction mechanism could invoke rate-determining activation energies, which would affect the observables. Because of the size of candidate species and potential complexity of the reaction mechanism, theoretical computations were focused only on the molecular structure and estimated reaction energetics. Structural parameters are given in Tables 2, 3, and 4 for dimers, trimers,

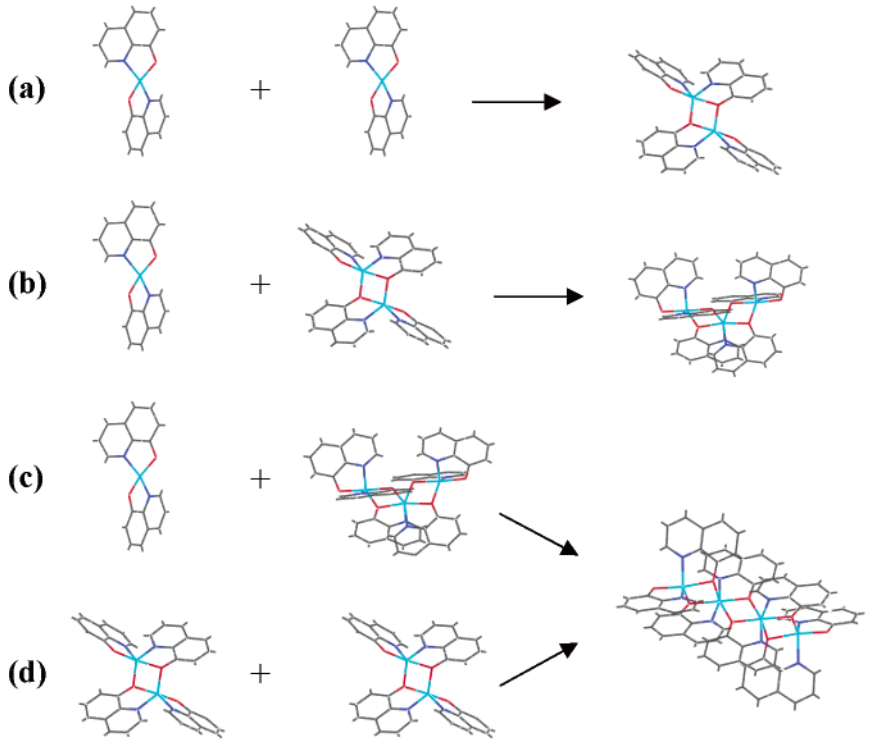

Figure 1. $(Znq_2)_x$ supramolecular structures formed by thermodynamically favorable oligomerization reactions between (a) 2 monomers to form a dimer, (b) monomer and dimer to form a trimer, (c) monomer and trimer to form a tetramer, and (d) 2 dimers to form a tetramer.

and tetramers, respectively. The corresponding atomic-labeled structures are shown in Figure 2.

3.1a. Monomers Znq_2 and $nMeq_2Zn$. The Znq_2 monomer is the fundamental building block for the $(Znq_2)_x$ oligomeric series. The monomeric form features the Zn center in a four-coordinate, distorted tetrahedral geometry (bond angles: O−Zn−O (131°); N−Zn−N (119.5°); O−Zn−N-chelate ring (86°); and O−Zn−N-between ligands (119.5°)) because of inequivalent bonding interactions between Zn−O and Zn−N. The Znq_2 monomer is the most polar oligomer in the series with a calculated dipole moment of 6.84 D. Methyl substitution of the pyridyl ring at C2 introduces steric hindrance, which causes a further distortion of the bond angles, increasing the N−Zn−N and O−Zn−O bond angles by 5−6° and decreasing the O−Zn−N bond angle between ligands by ∼5°, with no significant change in the O−Zn−N bond angle of the chelate ring or in bond lengths about the Zn center (Zn−O ∼1.87 Å and Zn−N ∼2.03 Å for all nMeq$_2$Zn monomers). Calculated dipole moments for the C2-, C4-, and C5-methylated Znq_2 monomers are 6.56, 7.23, and 6.98 D, respectively.

3.1b. Dimers $(Znq_2)_2$ and $(nMeq_2Zn)_2$. The dimeric form of Znq_2 is the first step in the oligomerization process toward building larger forms of Zn (8-quinolinolato) chelates (see Figure 1a). Electronic-structure calculations indicate that monomer dimerization would be energetically favorable in the gas phase by 52−54 kcal/mol for the parent and its methylated derivatives, with the exception of 2Meq$_2$Zn. For this latter case, C2 methylation ortho to the pyridyl nitrogen of the 8-quinolinol ligand causes steric repulsion effects, resulting in a distorted structure with decreased stability. Solvation effects were evaluated for a chloroform solution using the PCM model and were found to reduce the oligomerization energies by 10−25%. This suggests that the relative stability of the dimeric complex is decreased as a result of its dielectric surroundings. It is important to note that, while these energies in themselves are consistent with the dielectric effect observed in Hopkins work,[8] the PCM calculation can only assess the energies of a molecular conformation for a solute in solution. Specific interactions, adduct formation, and alternate pathways are not considered herein. Further, this current work uses gas-phase geometries for the PCM calculations. Continuing work in our group is exploring the effects of solvation induced structural relaxations and the effect of explicit nucleophilic interaction.

The Zn atoms in the parent Znq_2 dimer are both pentacoordinate, resulting in distorted trigonal bipyramidal geometries. The bond angles deviate from the ideal 90° (79−106.6°) and 120° (113.6−125°) bond angles, which is slightly more distorted compared to the Zn(BZT)$_2$ dimer crystal structure reported by Yu et al.,[18] and likely a consequence of the more rigid 8-quinolinol ligand and smaller chelation ring. Compared to the Znq_2 monomer, a single 8-quinolinol ligand from each Znq_2 species acts as an oxo bridge between the two Zn centers, creating the characteristic Zn−O core structure seen in the rest of the $(Znq_2)_x$ series. The Zn−O core structure features a Zn_2O_2 ring unit with Zn−O (bridging) bond lengths 1.93 and 2.12 Å and inner bond angles of 99.2 and 80.8°. These bond lengths and bond angles of the Zn_2O_2 ring unit are similar to those reported for the Zn(BZT)$_2$ dimer.[18] The distance between the two Zn ions is 3.09 Å. The Zn−N bonds lengths are close to the monomeric compound (2.02 Å), but the nonbridging Zn−O bonds of the dimer are longer by 0.1 Å.

Methyl substitution had negligible effect on the dimeric structures compared to $(Znq_2)_2$ with all structures exhibiting high symmetry and near-zero dipole moments. Slightly longer Zn−N bond lengths (∼0.05−0.1 Å) and shorter bridging Zn−O bond lengths (∼0.04−0.1 Å) were calculated for $(2Meq_2Zn)_2$, resulting in an increased distance between Zn atoms (3.14 Å).

3.1c. Trimers $(Znq_2)_3$ and $(nMeq_2Zn)_3$. The $(Znq_2)_3$ compound is the smallest oligomer containing Zn atoms with different coordination geometries. The central Zn atom (Zn1) in the trimer is hexacoordinate, and the two outer Zn atoms (Zn2) are both pentacoordinate. Oligomerization energies of the trimer are

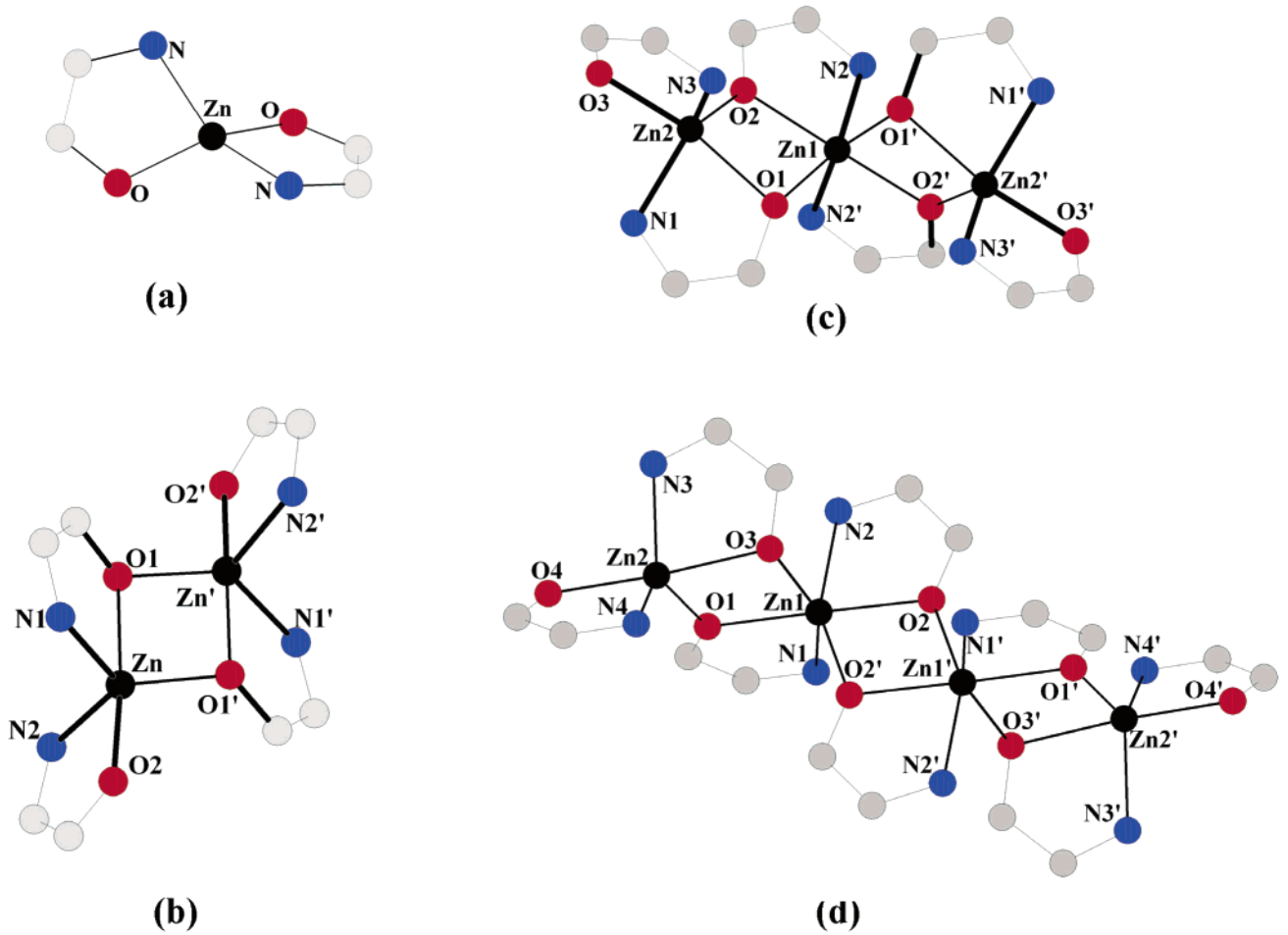

Figure 2. Structures showing the coordination geometry and atomic labeling about the Zn ions in the (a) monomer, (b) dimer, (c) trimer, and (d) tetramer for Znq_2. The full 8-quinolinolate ligands are not shown for clarity.

TABLE 2: Calculated Structural Parameters for (nMeq$_2$Zn)$_2$ Dimers

	(Znq_2)$_2$ and (nMeq$_2$Zn)$_2$, n = 4, 5[a]	(2Meq$_2$Zn)$_2$
	Bond Lengths (Å)	
Zn−O1′	1.93	1.97
Zn−O1	2.12	2.01
Zn−O2	1.97	1.96
Zn−N1	2.02	2.13
Zn−N2	2.03	2.08
	Bond Angles (deg)	
Zn−O1′−Zn′	99.3	104.4
O1′−Zn−O1	80.8	75.6
O2−Zn−01′	106.6	95.2
O2−Zn−01	172.6	167.7
O2−Zn−N2	83.1	82.9
O1−Zn−N2	95.5	108.1
O1′−Zn−N2	113.6	114.9
O2−Zn−N1	95.3	101.7
O1−Zn−N1	79.0	79.3
O1′−Zn−N1	125.0	131.7
N1−Zn−N2	118.8	112.0

[a] Differences in bond lengths are <0.01 Å and in bond angles are <0.2° compared to the unsubstituted derivative.

TABLE 3: Calculated Structural Parameters for (nMeq$_2$Zn)$_3$ Trimers

	(Znq_2)$_3$ and (nMeq$_2$Zn)$_3$, n = 4, 5[a]	(2Meq$_2$Zn)$_3$
	Bond Lengths (Å)	
Zn2−O1	2.11	2.02
Zn2−O2	1.91	1.96
Zn2−O3	1.99	1.96
Zn1−O1	2.02	2.02
Zn1−O2	2.06	2.05
Zn2−N1	2.04	2.09
Zn2−N3	2.04	2.13
Zn1−N2	2.16	2.21
	Bond Angles (deg)	
Zn2−O1−Zn1	96.5	102.7
Zn2−O2−Zn1	101.9	103.8
O1−Zn2−O2	80.4	77.5
O1−Zn1−O2	79.2	75.3
O1−Zn2−O3	169.2	172.3
O2−Zn2−O3	108.1	95.1
O2−Zn2−N3	113.4	127.3
O1−Zn2−N3	100.4	101.7
O2−Zn2−N1	122.1	119.3
N1−Zn2−N3	123.2	112.2
N2−Zn1−N2′	87.0	85.9

[a] Differences in bond lengths are <0.01 Å and in bond angles are <0.2° compared to the unsubstituted derivative.

generally smaller when compared to dimer formation (see Table 1). Solvation reduces these energies by 16−21% of their gas-phase values.

The octahedral geometry about Zn1 is distorted with bond angles deviating from the ideal 90° (79−95.2) with a 24° deviation from the ideal angle of 180° for the trans coordination sites. This distortion of the octahedral geometry about the central Zn atom was greater compared to the Zn(ppo)$_2$ trimer crystal structure reported by Kim et al.,[19] which is composed of more flexible ligands and a larger chelation ring (six-membered ring for Zn(ppo)$_2$ trimer vs five-membered ring for Znq_2 trimer).

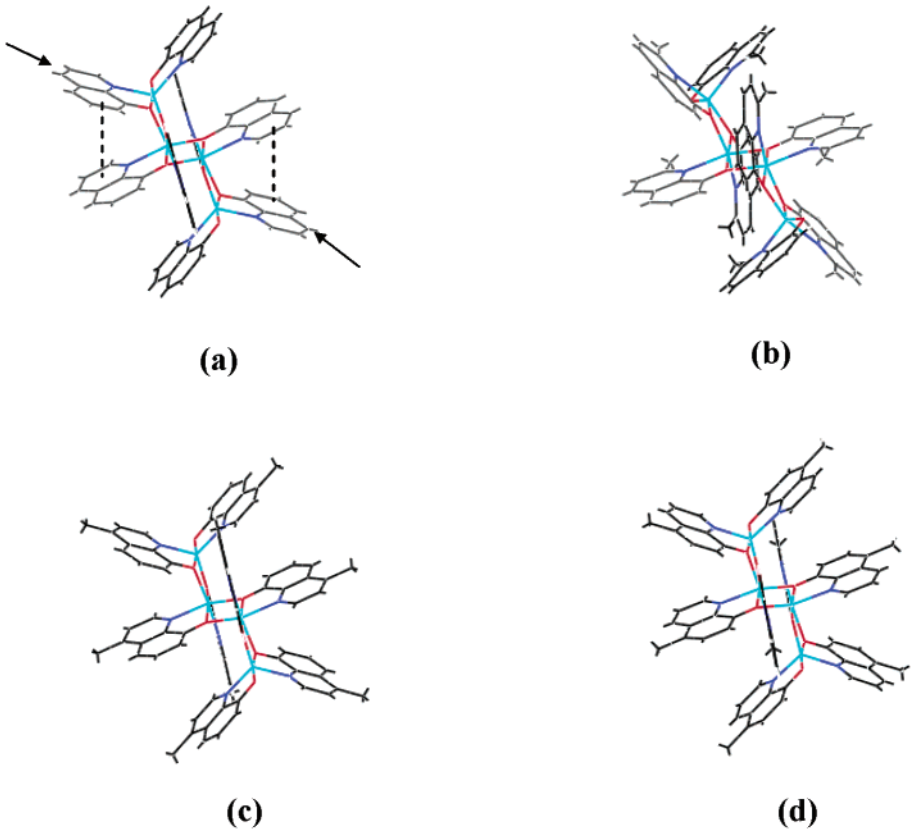

Figure 3. Calculated structures for (a) $(Znq_2)_4$, (b) $(2Meq_2Zn)_4$, (c) $(4Meq_2Zn)_4$, and $(5Meq_2Zn)_4$ tetramers showing distortion caused by introducing steric hindrance at the C2 position of the chelating ligand. Dotted lines show *intra*molecular $\pi-\pi$ stacking interactions, and arrows identify ligands involved in close *inter*molecular interactions, previously identified in $(Znq_2)_4$, and likely absent in $(2Meq_2Zn)_4$.

The trigonal bipyramidal geometry about the Zn2 ions is also distorted but more similar to the $Zn(ppo)_2$ trimer, with angles deviating from the ideal 90° (range of 78.8−113.4°) and 120° (∼123°) about the metal ion, similar to the calculated Znq_2 dimer structure, as are the Zn2−O and Zn2−N bond lengths. All Zn1−O bond lengths are ∼2.04 Å, and Zn1−N bond lengths are 2.16 Å, and the distance between Zn atoms is 3.08 Å.

Methylation of the 8-quinolinol ligand had little effect on the structural parameters of the calculated trimer structures. For $(2Meq_2Zn)_3$ steric hindrance causes a small lengthening of all Zn−N bonds by 0.05−0.1 Å with a corresponding shortening of the Zn2−O bonds by the same amount. However, the Zn1−O bond lengths are similar to the other derivatives. Unlike the symmetrical dimeric oligomers, the trimeric structures had nonzero computed dipole moments (0.65, 0.71, 0.52, and 0.66 D for $(Znq_2)_3$, C2, C4, and C5 methylated derivatives, respectively).

3.1d. Tetramers $(Znq_2)_4$ and $(nMeq_2Zn)_4$. The computed molecular structure of $(Znq_2)_4$ has been reported in previous work,[13] and results were consistent with experimental values.[12] There are two candidate-formation processes considered in this report: (1) the addition of monomeric Znq_2 to the trimeric species $[(Znq_2)_3]$ (Figure 1c) and (2) dimerization of dimeric Znq_2 $[(Znq_2)_2]$ (Figure 1d). As details of the reaction pathways with the relevant activation energetics have not been reported, both potential sources of tetrameric species formation were included. Both gas-phase and solution energetics are favorable for either process and are significantly reduced by 25−40% compared to the monomer dimerization energies.

The tetrameric compound of the parent Znq_2 species contains two central Zn atoms (Zn1) that are hexacoordinate and two outer Zn atoms (Zn2) that are pentacoordinate, as reported previously by Kai et al.[12] The bond angles and bond lengths about the Zn1 centers are similar to the Znq_2 trimer with resultant distorted octahedral geometries. There were no significant changes in the structural parameters for the Znq_2 tetramer upon methylation at the C4 and C5 positions, as seen in Table 4. However, steric hindrance effects of C2 methylation are mainly reflected in the bond lengths and corresponding bond angles of the terminal bridging ligands. In previous work for $(Znq_2)_4$, these terminal bridging ligands were shown to exhibit close inter- and intramolecular $\pi-\pi$ stacking interactions, where the latter are absent in the $2Meq_2Zn$ derivative (see Figure 3). This is mainly due to the lengthening of the Zn2−N3 bond by ∼0.2 Å, with a corresponding decrease in the Zn2−O3 bond length by ∼0.1 Å. As a result, the geometry about the Zn2 ions is more highly distorted from trigonal bipyramid compared to the other $nMeq_2Zn$ tetramers. These structural changes cause distortion about the Zn_2O_2 units in $(2Meq_2Zn)_4$, where distances between Zn1···Zn1′ are slightly larger (3.24 Å) compared to Zn1···Zn2 (3.19 Å). For the other $(nMeq_2Zn)_4$ chelates, the distances between Zn atoms are identical (3.13 Å).

3.2. Experimental Oligomeric Purity Determination by SEC. *3.2a. Size Evaluation.* The oligomeric purity of the $nMeq_2Zn$ chelates in solution was measured using SEC calibrated against MW standards. The polystyrene MW standards ST2330 and ST760 were chosen because the MW of the Znq_2 tetramer falls between these two values (1415 amu). Additional calculations of the molecular volumes (MV) and surface areas were conducted for the monomers, dimers, trimers, and tetramers of the $(nMeq_2Zn)_x$ series and compared to Alq_3 and are shown in Table 5. The ratios of the size differences between different oligomers of Znq_2 and Alq_3 using these parameters were calculated and tabulated (Table 6). On the basis of these

TABLE 4: Calculated Structural Parameters for (nMeq$_2$Zn)$_4$ Tetramers

	$(2Meq_2Zn)_4$	$(4Meq_2Zn)_4$	$(5Meq_2Zn)_4$
	Bond Lengths (Å)		
Zn1−O2	2.05	2.04	2.04
Zn1−O2′	2.02	1.98	1.98
Zn1−O3	2.05	2.05	2.05
Zn1−O1	2.04	2.07	2.07
Zn2−O1	2.01	1.91	1.91
Zn2−O3	1.97	2.10	2.10
Zn2−O4	1.95	1.99	1.99
Zn1−N1	2.24	2.16	2.17
Zn1−N2	2.23	2.18	2.19
Zn2−N3	2.20	2.03	2.03
Zn2−N4	2.07	2.03	2.04
	Bond Angles (deg)		
Zn1−O2−Zn1	105.4	102.2	102.2
Zn1−O1−Zn2	103.4	103.5	103.6
Zn1−O3−Zn2	105.2	97.9	97.8
O2−Zn1−O2′	74.6	77.8	77.8
O1−Zn1−O3	73.6	77.9	77.9
O1−Zn2−O3	76.1	80.3	80.3
O1−Zn2−N4	103.6	119.7	119.7
O3−Zn2−N4	128.9	100.1	100.1
O1−Zn2−N3	151.9	122.8	122.8
O3−Zn2−N3	78.5	79.6	79.6
N3−Zn2−N4	101.6	116.7	116.7
N1−Zn1−N2	85.3	84.6	84.6
O4−Zn2−N4	83.4	82.5	82.5

TABLE 5: Calculated MWs, MVs, and Surface Areas of (nMeq$_2$Zn)$_x$ Oligomers and Alq$_3$

property	$(Znq_2)_x$	$(2Meq_2)_xZn$	$(4Meq_2)_xZn$	$(5Meq_2)_xZn$	Alq_3
		MW (amu)			
monomer	353.69	381.74	381.74	381.74	459.44
dimer	707.37	763.48	763.48	763.48	
trimer	1061.06	1145.22	1145.22	1145.22	
tetramer	1414.74	1526.95	1526.95	1526.95	
		MV (Å^3)			
monomer	847.7	915.8	934.4	935.2	1154.9
dimer	1519.8	1664.5	1706.2	1712.4	
trimer	2117.0	2300.5	2393.3	2394.7	
tetramer	2699.9	2891.6	3067.9	3070.3	
		Surface Area (Å^2)			
monomer	517.1	542.3	562.5	564.3	656.6
dimer	833.2	877.0	927.2	912.1	
trimer	1056.4	1083.1	1195.5	1195.3	
tetramer	1259.7	1274.6	1441.9	1440.8	

TABLE 6: Size Ratios of $(Znq_2)_x$ Oligomers and Alq$_3$ Based on Calculated MWs, MVs, and Surface Areas

oligomer comparison	ratio of MWs	ratio of MVs	ratio of surface areas
$(Znq_2)_4/(Znq_2)_3$	1.3	1.3	1.2
$(Znq_2)_3/(Znq_2)_2$	1.5	1.4	1.3
$(Znq_2)_2/Znq_2$	2.0	1.8	1.6
$(Znq_2)_2/Alq_3$	1.5	1.3	1.3
Alq_3/Znq_2	1.3	1.4	1.3

calculations, the differences in MV and surface area of the Znq_2 oligomers scale in proportion to the differences in MW. Alq_3 is ~1.3 times larger in size than the Znq_2 bischelate. These results suggest that separation of these metal chelates according to size is feasible.

3.2b. SEC Results. The size-exclusion chromatograms for ST760, ST2330, Alq_3, and 8-quinolinol obtained using $CHCl_3$ as the mobile phase are shown in Figure 4a. A single peak was observed for both Alq_3 and 8-quinolinol with retention times longer (15.1 and 20.3 min, respectively) than the smaller MW standard ST760 (13.1 min), indicating a good correspondence to the smaller size and MWs (459.4 and 145.16, respectively)

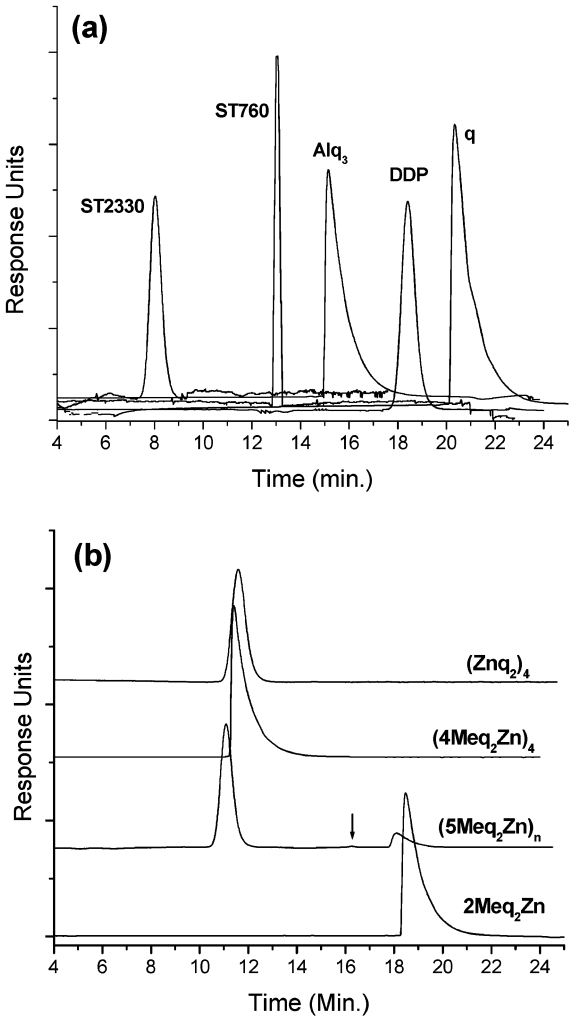

Figure 4. Chromatograms of (a) polystyrene standards, Alq_3, DDP, and 8-quinolinol and (b) the crystalline nMeq_2Zn chelates. Arrow identifies a third peak observed for $5Meq_2Zn$. All samples were dissolved in $CHCl_3$ and run under identical conditions.

of the reference materials. The MW standard ST2330 appeared at the shortest retention time (8.05 min) and gave a broader peak because of a larger polydispersity compared to ST760.

Although "tailing" of both the Alq_3 and q peaks was observed, there was no evidence for decomposition of the metal chelate on the column. The asymmetry of a peak cannot be directly related to a specific process, but molecular interaction phenomena are known to influence the shape.[27] For example, functional groups left on the column after manufacture can interact with the injected sample and cause tailing. The oxygen atom of 8-hydroxyquinoline is a possible site of interaction with the column. To test this possibility 2,9-dimethyl-4,7-diphenyl-1,10-phenanthroline (DDP) (360.46 amu), which does not have any oxygen atoms, was tested on the column and the chromatogram is shown in Figure 4a. This sample gave a single peak with very little tailing compared to Alq_3 or the ligand, suggesting that the phenolic oxygen may have some interaction with the column.

The chromatograms of the crystalline nMeq$_2$Zn chelates dissolved in $CHCl_3$ are shown in Figure 4b. The unsubstituted zinc chelate exhibited a single peak at a retention time between the ST2330 and ST760 MW standards consistent with a tetrameric structure and in agreement with previous experimental results[13] and energetic calculations presented here. Single peaks were also observed for crystalline $4Meq_2Zn$ and $2Meq_2Zn$ at

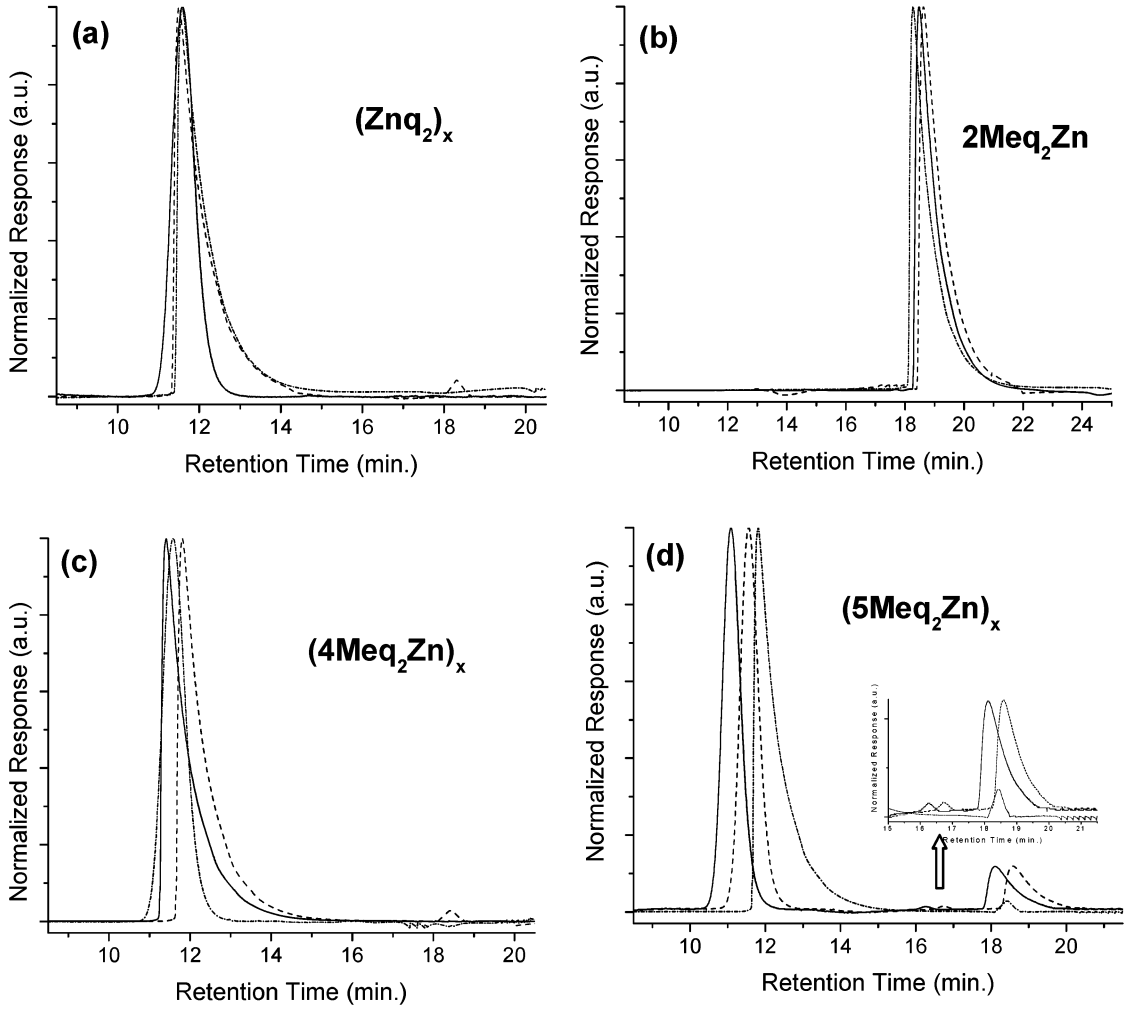

Figure 5. Comparison of the chromatograms for (a) $(Znq_2)_4$, (b) $2Meq_2Zn$, (c) $4Meq_2Zn$, and (d) $5Meq_2Zn$ prepared as crystalline materials dissolved in $CHCl_3$ (solid line), as crystalline materials dissolved in $CHCl_3$ with 10 μL DMSO (dashed line), and vapor-deposited films dissolved in $CHCl_3$ (dot-dot-dashed line). The chromatograms were normalized to the major peak.

retention times of 11.6 and 18.5 min, respectively. The $4Meq_2Zn$ retention time was similar to $(Znq_2)_4$, suggesting that $4Meq_2Zn$ is also likely tetrameric. In contrast, the much longer retention time observed for $2Meq_2Zn$, which appeared between the retention times for Alq_3 and q, suggests that $2Meq_2Zn$ is monomeric, at least in solution. These results support previous photophysical studies of the *n*Meq_2Zn series, where $2Meq_2Zn$ was suggested to be monomeric because it showed solvent-dependent absorption properties consistent with a more polar bischelate.[15,16]

The $5Meq_2Zn$ chelate was unique in the zinc chelate series because three peaks (11.1, 16.1, and 18.1 min) were detected, as seen in Figure 4b, suggesting either that more than one oligomeric species was present in the crystalline solid or that the chelate disassociated in $CHCl_3$. The first peak eluted off the column near the retention time for the tetramer and was the most prominent peak, indicating a greater concentration of this oligomeric species. The third peak was detected at a retention time similar to $2Meq_2Zn$, suggesting that some of the $5Meq_2Zn$ chelate exists in the monomeric form. The second peak was the smallest eluting from the column at 16.1 min, which falls between the retentions times identified for the tetramer and monomer. However, this retention time is longer compared to Alq_3 and is inconsistent with either a dimer or trimer species, both of which should elute earlier than Alq_3 based on the size analysis (see Tables 5 and 6). Therefore the possibility of an impurity or some other transitional form of the zinc chelate species cannot be ruled out. Several aliquots of $5Meq_2Zn$ were run through the column and eluting species collected. Analysis of the sample eluting at ~18 min exhibited characteristic fluorescence of the $5Meq_2Zn$ tetramer, consistent with previous reports.[16] However, the minimal sample size of peaks eluting at longer retention times prevented further analysis of these species.

3.2c. Effect of Sample Preparation on SEC Results. The stability of the Znq_2 tetramer to nucleophilic solvents and to thermal vapor deposition to form thin films was also evaluated. SEC data were collected for *n*Meq_2Zn chelates and Alq_3 as crystalline samples dissolved in $CHCl_3$ with DMSO added and as amorphous samples (thin films) dissolved in $CHCl_3$.

The normalized chromatograms for the *n*Meq_2Zn series analyzed under different sampling conditions are shown in Figure 5 and the number of peaks and retention times are summarized in Table 7. No significant changes in the SEC results were observed for Alq_3 or $2Meq_2Zn$ under the different sampling conditions. However, a new peak at a retention time of ~18.4 min was observed for both Znq_2 and $4Meq_2Zn$ with the addition of DMSO, suggesting that, in agreement with Hopkins, the tetramer partially dissociates to the monomeric form in the presence of DMSO.[8] The samples prepared from vapor-deposited films of Znq_2 and $4Meq_2Zn$ showed similar SEC results in $CHCl_3$ compared to the crystalline materials, suggesting that the tetrameric structure is stable to thermal sublimation conditions.

TABLE 7: Summary of Retention Times (min) under Different Sampling Conditions

sample	crystalline ($CHCl_3$)	crystalline ($CHCl_3$+DMSO)	amorphous film ($CHCl_3$)
ST2230	8.0	8.0	
ST760	13.1	13.1	
8-quinolinol	20.3	20.3	
Alq_3	15.1	15.1	15.1
$(Znq_2)_x$	11.6	11.5, 18.3	11.6
$2Meq_2Zn$	18.5	18.6	18.3
$(4Meq_2Zn)_x$	11.4	11.8, 18.4	11.6
$(5Meq_2Zn)_x$	11.1, 16.1, 18.1	11.5, 16.7, 18.5	11.8, 18.4

In the case of $5Meq_2Zn$, addition of DMSO had little effect on the number or relative sizes of peaks. Three peaks were observed, but all slightly shifted to longer retention times compared to the crystalline sample dissolved in $CHCl_3$ only. However, the chromatogram for the thin-film sample showed a reduction in size of the peak at ~18 min and no peak at 16 min, suggesting that the tetramer is dominant in the vapor-deposited film but may still contain the monomer as a mixture.

4. Discussion

The complimentary nature of the computational and SEC results allows us to make several observations regarding the stable solution form(s) of the Zn (8-quinolinolato) chelate and its related methyl substituted derivatives. The computed energetics for oligomer formation favor the formation of larger-sized compounds, in both gas- and solution-phase conditions. Methyl substitution affects these energetics to a lesser degree than solvation effects. Although the largest-sized oligomer was the tetramer, structural parameters (bond lengths and bond angles) of the Zn−O core structure do not change significantly as the oligomer increases in size, and the exothermic energetics would suggest that even larger oligomers are possible. However, solubility limits beyond tetramers prohibit synthesis in solution.

The SEC results are generally in agreement with these computational results in that the major components in $CHCl_3$ solution for the parent, $4Meq_2Zn$, and $5Meq_2Zn$ were the tetrameric species. SEC results show that $2Meq_2Zn$ is a monomer in all solvent systems, which is consistent with the computed lower stability of the tetrameric form compared to the other derivatives in the series. However, no conclusive evidence of the nature of the oligomeric form of $2Meq_2Zn$ in the solid state (i.e., both crystalline and thermally vapor-deposited films) can be concluded based on SEC results alone. Solid-state characterization by ^{13}C cross polarization magic-angle spinning NMR spectroscopy and X-ray diffraction of these materials will aid in further understanding their structures in the solid state.

The addition of DMSO to the chloroform solutions allowed us to examine the effect of nucleophilic agents, a mixed solvent condition not tested by the computational results reported here. The appearance of smaller oligomers for the parent and $4Meq_2Zn$ tetrameric compounds demonstrates that the reaction mechanism for oligomer formation is affected by the presence of nucleophilic species. However, these results also suggest that the breakdown of the tetrameric structure may not be simply a function of the presence of a nucleophilic agent (DMSO). The absence of changes in the SEC results for the $5Meq_2Zn$ tetrameric derivative with the addition of DMSO would suggest that a more complete examination of the effects of nucleophilic agents on these compounds is necessary to discern the reaction mechanism of Zn (8-quinolinato) species.

Such results demonstrate that care must be exercised when using molecular parameters measured in solution as indicators of the properties of a thin-film material. The measurement conditions, solid-state or solution, affect the supramolecular structure of Znq_2 and its derivatives and may impact interpretations of charge transport in these materials. Since dipolar dispersion is expected to affect both the bulk transport[14] and charge injection[28] properties of an OLED, understanding the structure of these materials *in the thin-film form* is critical in order to develop structure−property relationships and to move toward design rules for optimizing both charge injection and transport to achieve lower-voltage small-molecule OLEDs. The presence of smaller oligomers (polar monomers) would affect the dipolar dispersion in solid-state films, even at relatively low levels of concentration.

5. Conclusions

A combination of SEC and electronic-structure calculations were used to determine the oligomeric form(s) of Zn (8-quinolinolato) chelates and their dependency on solid-state and solution conditions. The supramolecular structures of Znq_2 and its derivatives vary between solution and solid state and between solvents of different nucleophilic strength, and these variations are strongly affected by methylation of the 8-quinolinol ligand. While the unsubstituted Zn (8-quinolinolato) chelate forms a supramolecular tetrameric structure with a single-crystal phase and methylation at the C4 position also yields a stable tetramer, methylation at the C2 position results in monomers in solution and methylation at the C5 position appears to result in a range of stable oligomers. The calculated near-zero dipole moments of the tetrameric structures are expected to eliminate dipolar disorder effects in vapor-deposited films, which may be one reason for lower operating voltages in OLEDs incorporating electroluminescent Znq_2 chelates. Overall, our results caution that solution-derived parameters cannot be directly applied to solid-state device performance (for example, the use of oxidation and reduction potentials measured using cyclic voltammetry to estimate unoccupied and occupied states in the solid film). Such connections may be rendered inaccurate if the supramolecular structure of the material changes in different solvents or between solution and solid state. If the solubility limit can be overcome, e.g., synthesis from the vapor phase, energetics suggest even larger oligomers are possible.

Acknowledgment. The authors gratefully acknowledge financial support from NSF (CAREER-DMR-9874765), Office of Naval Research (N00014-03-1-0247), Office of Basic Energy Sciences, U. S. Department of Energy, and the Pacific Northwest National Laboratory (PNNL) Laboratory Directed Research and Development Program. PNNL is operated by Battelle Memorial Institute for the U.S. Department of Energy under Contract DE-AC06-76RLO 1830.

Supporting Information Available: All calculated structural coordinates for the full $(n Meq_2Zn)_x$ series. This material is available free of charge via the Internet at http://pubs.acs.org.

References and Notes

(1) Tang, C. W.; VanSlyke, S. A. *Appl. Phys. Lett.* **1987**, *51*, 913.

(2) Brinkmann, M.; Gadret, G.; Muccini, M.; Taliani, C.; Masciocchi, N.; Sironi, A. *J. Am. Chem. Soc.* **2000**, *122*, 5147.

(3) Kushto, G. P.; Iizumi, Y.; Kido, J.; Kafafi, Z. H. *J. Phys. Chem.* **2000**, *104*, 3670.

(4) Burrows, P. E.; Sapochak, L. S.; McCarty, D. M.; Forrest, S. R. Thompson, M. E. *Appl. Phys. Lett.* **1994**, *64* (20), 2718.

(5) Curioni, A.; Boero, M.; Andreoni, W. *Chem. Phys. Lett.* **1998**, *294*, 263.

(6) Martin, R. L.; Kress, J. D.; Campbell, I. H.; Smith, D. L. *Phys. Rev. B* **2000**, *61*, 15804.
(7) Sapochak, L. S.; Padmaperuma, A.; Washton, N.; Endrino, F.; Schmett, G.; Marshall, J.; Fogarty, D.; Burrows, P. E.; Forrest, S. R. *J. Am. Chem. Soc.* **2001**, *126*, 6500.
(8) Hopkins, T. A.; Meerholz, K.; Shasheen, S.; Anderson, M. L.; Schmidt, A.; Kippelen, B.; Padias, A. B.; Hall, K. H.; Peyghambrian, N.; Armstrong, N. R. *Chem. Mater.* **1996**, *8* (2), 344.
(9) Cölle, M.; Gmeiner, J.; Milius, W.; Hillebrecht, H.; Brütting, W. *Adv. Funct. Mater.* **2003**, *13*, 108.
(10) Ferris, K. F.; Sapochak, L. S.; Rodovsky, D.; Burrows, P. E. *Proc. Mater. Res. Soc., Org. Polym. Mater. Devices* **2003**, *771*, L3.3.
(11) Braun, M.; Gmeiner, J.; Tzolov, M.; Coelle, M.; Meyer, F. D.; Milius, W.; Hellebrecht, H.; Wendland, O.; von Schutz, J. U.; Brutting, W. *J. Chem. Phys.* **2001**, *114*, 9625.
(12) Kai, Y.; Moraita, M.; Yasuka, N.; Kasai, N. *Bull. Chem. Soc. Jpn.* **1985**, *58*, 1631.
(13) Sapochak, L. S.; Bennicasa, F.; Schofield, R.; Baker, J.; Riccio, K.; Fogarty, D.; Kohlmann, H.; Ferris, K. F.; Burrows, P. E. *J. Am. Chem. Soc.* **2002**, *124*, 6119.
(14) Parris, P. E.; Kendre, V. M.; Dunlap, D. H. *Phys. Rev. Lett.* **2001**, *87*, 126601.
(15) Endrino, F. M.S. Degree in Chemistry, University of Nevada, Las Vegas, 2001.
(16) Sapochak, L. S.; Endrino, F.; Marshall, J.; Fogarty, D.; Washton, N.; Nanayakkara, S. In *Molecules as Components of Electronic Devices*, Lieberman, M., Ed.; ACS Symposium Series 844; American Chemical Society: Washington, DC, 2003; pp 171−186.
(17) Van der Schaaf, P. A.; Wissing, E.; Boersma, J.; Smeets, W. J. J.; Spek, A. L.; van Koten, G. *Organometallics* **1993**, *12*, 3624.
(18) Yu, G.; Yin, S.; Shuai, Z.; Zhu, D. *J. Am. Chem. Soc.* **2003**, *125*, 14816.
(19) Kim, T. S.; Okubo, T.; Mitani, T. *Chem. Mater.* **2003**, *15*, 4949.
(20) Schmidt, M. W.; Baldridge, K. K.; Boatz, J. A.; Elbert, S. T.; Gordon, M. S.; Jensen, J. J.; Koseki, S.; Matsunaga, N.; Nguyen, K. A.; Su, S.; Windus, T. L.; Dupuis, M.; Montogomery, J. A. *J. Comput. Chem.* **1993**, *14*, 1347.
(21) Binkley, J. S.; Pople, J. A.; Hehre, W. J. *J. Am. Chem. Soc.* **1980**, *102*, 939.
(22) Dobbs, K. D.; Hehre, W. J. *J. Comput. Chem.* **1987**, *8*, 861.
(23) Miertus, S.; Scrocco, E.; Tomasi, J. *J. Chem. Phys.* **1981**, *55*, 117.
(24) Tomasi, J.; Presico, M. *Chem. Rev.* **1994**, *94*, 2027.
(25) Barone, V.; Cossi, M.; Mennucci, B.; Tomasi, J. *J. Chem. Phys.* **1997**, *107*, 3210.
(26) Tomasi, J.; Mennucci, B.; Cances, E. *THEOCHEM* **1999**, *464*, 211.
(27) Heineman, W. R.; Strobel, H. A. *Chemical Instrumentation: A Systematic Approach*; John Wiley & Sons: New York, 1989.
(28) Baldo, M. A.; Forrest, S. R. *Phys. Rev. B* **2001**, *64*, 085201.